Escola de Camins

Escola Tècnica Superior d'Enginyeria de Camins, Canals i Ports

UPC BARCELONATECH

SPECTRAL ANALYSIS OF WATER CONTENT CHANGES IN AN UNSATURATED SOIL LAYER

Trabajo realizado por:

Emeric Fuentes Vásquez

Dirigido por:

Jean Vaunat

Yeudy Vargas Alzate

Máster en:

Ingeniería del Terreno

Barcelona, Septiembre 2022

Departamento de Ingeniería Civil y Ambiental

TRABAJO FINAL DE MASTER

Acknowledgments

I'd like to express my appreciation to Jean Vaunat and Yeudy Vargas for their patience, wisdom, and invaluable expertise throughout this endeavour.

Thank you to my family for believing in me and providing me with this opportunity. Special thanks to my mother for her unfailing affection.

To my friends, here and there, for their endless patience, help, and concern; and, last but not least, to me.

Abstract

Shallow landslides seated in the unsaturated zone are mostly triggered by soil partial of total saturation and the prediction of the changes of water content in the vadose zone is fundamental for the estimation of landslide hazard. However, the simulation of the full coupled thermo-hydraulic processes taking place in the vadose zone under climatic actions require long and computationally costly numerical computations. This thesis seeks to use a Reduced order Model based on the spectral analysis as a cheap alternative for the prediction water content fluctuations. To this aim, two Soil Transfer Function are determined. The first one bis statistical and based on correlations between water content measurement at depth and at soil surface. The second is deterministic and based on an analytical solution of the one-dimensional infiltration equation under period water content/pressure variations at soil-atmosphere interface. Both approaches are validated on a set of monitored data obtained in an experimental field. Results shown that the estimation of water content using a deterministic soil transfer reached higher accuracy provided that the procedure is trained on a sub-set of measurements in order to determine characteristics values for the equation control parameters (length of the column, diffusion coefficient).

Keywords: Unsaturated sois, water infiltration, soil-atmosphere interaction, spectral analysis, water content prediction

Resumen

Los deslizamientos superficiales localizados en la zona no saturada ocurren en su mayoría por la saturación parcial o total de la zona vadosa y la predicción de los cambios de contenido de agua en la zona vadosa es fundamental para la estimación de la amenaza asociada a este tipo de deslizamientos. Sin embargo, la simulación de los procesos acoplados termo-hidráulicos que tienen lugar en la zona vadosa bajo acciones climáticas requiere cálculos numéricos largos y computacionalmente costosos. Esta tesis busca utilizar un Modelo de Orden Reducido basado en el análisis espectral como una alternativa económica para la predicción de fluctuaciones del contenido de agua. Para ello se determinan dos Funciones de Transferencia del Suelo. La primera es estadística y se basa en correlaciones entre mediciones de contenido de agua en profundidad y en superficie del suelo. La segunda es determinista y se basa en una solución analítica de la ecuación de infiltración unidimensional bajo variaciones periódicas de contenido/presión de agua en la interfase suelo-atmósfera. Ambos enfoques se validan en un conjunto de datos monitoreados en un campo experimental. Los resultados muestran que la estimación del contenido de agua mediante la función de transferencia determinista alcanza una mayor precisión siempre que un procedimiento de back-análisis de los valores característicos de la ecuación (longitud de la columna, coeficiente de difusión) se realiza en un subconjunto de los datos monitorizados.

Palabras clave: Suelo no saturado, infiltración de agua, interacción suelo-atmósfera, análisis espectral, predicción del contenido de agua

Contents

List of Figures

1 CHAPTER: INTRODUCTION

1.1 Introduction

Landslides, soil-cracking and deformations in the ground due climate change has become an important topic to analyse. About 33% of the earth's surface is considered arid or semiarid [1]. This percentage is growing considerably with the climate change and temperatures rising every year. As a result, the stresses of the soil changes and pore pressures associated to more significant events of intense rainfall can cause numerous slope failures.

Studying the interaction between the atmospheric conditions and the soil surface can help to recreate the physics phenomena in the ground. Moisture and thermal flux are major factors in variations in soil saturation, together with the properties of the ground surface and evapotranspiration from the vegetation cover. These strongly coupled phenomena require the use of numerical tool for a precise assessment of ground hydraulic state at any time.

However, the necessity to account for long duration time series of climatic actions, dense mesh close to soil-atmosphere interface and long previous history to determine the initial hydraulic state of the soil make numerical calculations extremely costly form the computational point of view [2].

In front of that, the use of a Reduced Order Model based on spectral analysis of soil water content provide an alternative to estimate long-term water content periodic variations in a cheapo way. As water content and pressure largely control slope shallow failure through changes in effective, the probability for these variables to reach a upper limit can further be used to estimate slope failure hazard. An example of the use of Reduced Order Model for hazard estimation purposes is presented by Giritana and Fredlund (2003b) [3], who proposed an "weather hazard model" that uses decision analysis for embankments. The dynamic programming optimization technique was used for the determination of critical slope stability conditions and the system was represented by PDEs governing water flow and stress conditions. [4].

This work presents preliminary evidences about the interest to use spectral analysis to assess hydraulic response of the vadose zone under climatic conditions. Vadose zone corresponds to the unsaturated soil layer in contact with the atmosphere and where most of ground water

content and pressure occur [5]. Pore-water pressures along the unsaturated zone can reach a maximum tension of -1GPa [6] while degree of saturation can varies from 100% to 0.

Two different methods are presented. The first method is based on developing a statistical soil transfer function (SFT) by linking variations in water content at the target depth to variations in water content at the soil surface. Once determined on the basis of a restricted period of the time series, the transfer function is used to predict the variation of water content at the relevant depth throughout the remainder of the series. This procedure will be repeated at each depth of water content measurement.

The second method involves calculating a deterministic SFT using the analytical solution to the one-dimensional infiltration problem described in Chapter 2. The analytical solution takes a constant diffusion coefficient into account, as well as two boundary conditions: a periodic sinusoidal boundary condition at the top of the one-dimensional soil column and a null water content at the bottom. Parameters involved in the analytical solution are optimized during the procedure in order to determine the diffusion coefficient of the soil and achieve the lowest estimation error.

1.2 Objectives

The primary objective of this thesis is to use spectral analysis for the analysis of water content fluctuations under climatic actions in order to reduce computation complexity and find correlation between shallow and underground water. For that, the following point must be tacked:

- Derivation of the infiltration equation from mass conservation equation, constitutive Darcy's law, and retention curve theory
- Determination of Soil Transfer function (SFT) to estimate the water content at any given time throughout the depth of a one-dimensional soil column.
- Solve the partial differential equation for specific boundary and initial conditions that represent the water content in a soil column due environment exposition.
- Computed the SFT and quantify the error estimation with recorded data from an experimental field located at Midi-Pyrénées – France.
- Compare the statistical SFT with the deterministic SFT

1.3 Methodology

This study aims to employ two reduced model techniques to quickly estimate soil water content profiles affected by climate changes.

In a first step, a statistical analysis of the correlation existing between water content variations at depth and in surface is carried out to set data-driven Soil Transfer Function (SFTs) and validate them.

In a second step, the statistical SFTs are compared with SFT outcoming from the analytical solution of the infiltration equation. This equation simulates water movement through the soil using the water mass balance, Darcy's law, and retention curve. The boundary conditions considered for the analytical solution of the PDE are the periodic fluctuation of water at soil surface, controlled by the soil-atmosphere interactions and a fixed water pressure (or water content) at the bottom of a one-dimensional soil column, corresponding to the presence of the phreatic level.

In a third step, both SFTs are validated on water content recordings during 7 years from an experimental horizontal field located at 'Le Fauga", France.

The results of this study show both approaches present a feasible alternative to precisely estimate time variation of water content within the vadose zone with low computing complexity and time calculations.

2 CHAPTER: BASIC CONCEPTS

Water flow in undeformable soil deposit is controlled by the equation that generally governs multi-phase flow in porous media. The objective of this chapter is to present the physical aspect and derive the equation for the case of a one dimensional soil layer.

2.1 One dimensional flow in Unsaturated Soil.

Numerous situations can be represented with a water flow mainly in one direction. If it is considered a ground surface with a phreatic level at a specified depth, the distribution of water will be as shown in the Figure 2-1.
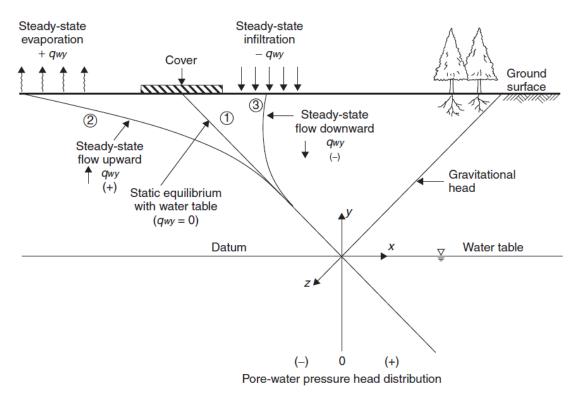
Figure 2-1. Hydrostatic equilibrium and steady-state flow conditions in zone negative pore water pressures [4]

From the water table to the surface, pore pressure and water content distribute linearly with depth, and the pore pressure follows the gravitational head magnitude relative to the phreatic level, as shown in Figure 2-1 with the line 1. This means that the hydraulic head is zero along the one-dimensional soil profile.

When there is no gradient of hydraulic head, there is no flow of water in vertical direction.

Scenario represented with line 1 does not result realistic when the soil is exposed to the environment because there are always changes of degree of saturation at the surface level.

Therefore, when it is considered changes at the surface of the ground profile, these will produce flow in vertical direction and subsequently changes at the linear pore pressure distribution.

Steady state infiltration will cause a water flow downward. The negative pore pressure distribution moves to the equilibrium moving from a positive value at the surface to zero at the water level, represented with line 3 at Figure 2-1. In case there is a positive water flow, which means, water moving upwards, hydraulic head changes to a more negative value at the surface when at the bottom keeps in zero (in contact with the water level) as is shown with line 2 on the Figure 2-1.

For these two described scenarios, when there is a water flow and consequently, changes in pressure and water content, it is expected that the diffusion equation can reproduce the changes throughout the soil column.

Hence, it results necessary to define the borders for the problem and for this hypothetical analysis, ground surface will work as the upper border, and the water table will represent the lower edge.

At the upper border, it will be applied the boundary condition that represents the interaction between the initial condition and the environmental conditions along time. As it will be shown further in this document, Fourier series function can be used to decompose the conditions in superimposable modes, either in terms in water content and pore pressure.

To represent the physical phenomena described with partial differential equations (PDE), specifically diffusion equation, the boundary conditions will be like hydraulic heads imposed at the upper level and known as Dirichlet boundary conditions whereas flow rates specified across the boundary or Neumann boundary conditions.

2.2   Application to the analysis of water content variations in a horizontal ground

The term of "soil-water balance" was introduced by Blight (1997) that represents the interaction flux of mass between the atmosphere and the ground.

Water flow influences evapotranspiration on the ground, but larger temperature gradients can also influence the thermo-mechanical response of a slope. [7].

Environmental conditions interact either at the surface or inside the ground. These processes generate a change of different variables including water content θ_w.

Environmental processes are classified as:

Thermal process	Moisture process	Air mass motion
• Direct solar radiation	• Cloud formation	
• Change of atmosphere temperature by radiation	• Precipitations	
• Atmosphere radiation (long wave)		

And these processes affect ground water because of the following effects:

Thermal process	Moisture process	Air mass motion
• Short wave ground reflection	• Run-off and ponding	• Wind effect
• Change of ground temperature by heat absorption	• Change in ground water content due to infiltration	
• Ground radiation	• Evaporation	
• Heat exchange due to ground-air temperature difference		
• Heat convected by water flow		

The interaction between environmental conditions and inside and outside processes is represented by Figure 2-2.
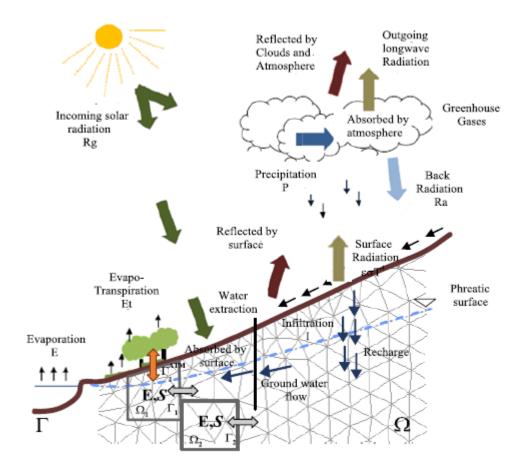
Figure 2-2: Fluxes of the "Soil-Water-Energy Balance", [8] [9]

2.3   Water infiltration or water content equation

The diffusion equation represents the process by which matter is transported from one part of a system to another as result of a random molecular motion [10]

As mentioned above, physical behaviour of an unsaturated-saturated soil mass can be deducted from the conversation mass principal which completed with the constitutive behaviour for water flow law and water storage law, such as the Retention Curve, ends in a partial differential equation for saturated-unsaturated liquid flow along the one-dimensional soil column.

A general form of the PDE for a one-dimensional case is,

$$k_{wz} \frac{\partial^2 h_w}{\partial z} + \frac{\partial k_{wx}}{\partial z} \frac{\partial h_w}{\partial z} = m_w \rho g \frac{\partial h_w}{\partial t} \qquad (2\text{-}1)$$

Where,

h_w: hydraulic head,

k_{wz}: water coefficient of permeability in the direction z which is in function of soil suction,

$\partial h_w / \partial z$: hydraulic head gradient in the x-direction,

ρ_w: density of water,

g: acceleration due gravity,

t: time, and

m_w: water storage coefficient which is a function of soil suction.

Considering a constant coefficient of water permeability, expression (2-1) reads:

$$k_{wz} \frac{\partial^2 h_w}{\partial z} = m_w \rho g \frac{\partial h_w}{\partial t} \qquad \text{(2-2)}$$

2.3.1 Phases of unsaturated soil

An unsaturated soil is formed by the solid, water and air phase. These three phases get represented on the Figure 2-3

Density and specific volume are used to define the volume-mass relationship property of each phase. The density of the soil particles ρ_s is defined by:

$$\rho_s = \frac{M_s}{V_s} \qquad \text{(2-3)}$$

Where:

M_s: mass of solids

V_s: volume of solids.

Specific gravity is defined as the ratio of solid particle density to water density ρ_W at 4°C (see (2-4)).

$$G_s = \frac{\rho_s}{\rho_w} \qquad (2\text{-}4)$$

Figure 2-3.shows the phase diagram in a unsaturated material. According to it, porosity *n* and degree of saturation S_r reads:

$$n = \frac{V_v}{V}, S_r = \frac{V_w}{V} \qquad (2\text{-}5)$$

Finally, the mass of water per unit volume of soil takes the form:

$$m_v = \rho_w n S_r \qquad (2\text{-}6)$$
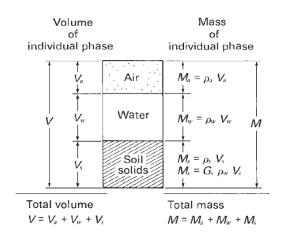
Figure 2-3. Distribution of the three different phases in a soil sample. [4]

Where,

V_w (L^3) : Water volume

V_s (L^3) : Solid particles volume.

V_v (L^3) : Void volume.

V (L^3) : Total volume

2.3.2 Water mass balance

Conservation water mass balances states that the inflows to any water systems or area is equal its outflow plus change in storage during a time interval.
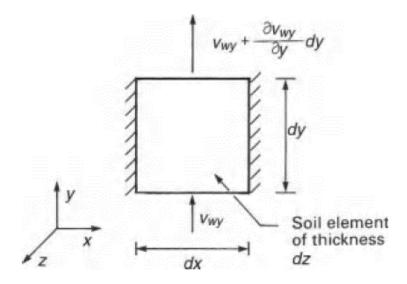
Figure 2-4. Water flow through a one-dimensional unsaturated soil element. [4]

Considering a non-deformable medium and without a source sink, as shown in Figure 2-4, the equation of conservation of the water mass is defined as,

$$\left(v_{wy} + \frac{dv_{wy}}{dy} dy \right) dxdz - v_{wy} dxdz = 0 \tag{2-6}$$

Where:

v_{wy} : water flow rate across a unit area of the soil in y direction,

dx, dy, dz : dimensions in x, y, and z respectively.

One-dimensional seepage can be derived by considering the continuity for the water phase. The assumption is that there are no changes with the total stress in the analysis, and then, the net flux of water through an element of unsaturated soil, in the z-direction, can be calculated from (2-7)

$$\frac{\partial \left(\frac{V_w}{V_0} \right)}{\partial t} = \frac{\partial v_{wz}}{\partial z} \tag{2-7}$$

Where:
V_w: volume of water in the element

V_0: initial overall volume of the element

$\partial \left(\frac{V_w}{V_0} \right) / \partial t$: rate of change in the volume of water in the soil element with respect to the initial volume of the element.

Then, in an element of unsaturated soil, net flux of water is the volume rates entering and leaving the element during a period of time.

For any change of V_w in time, V_w is represented by the water retention curve in terms of the volumetric water content when calculating water storage.

2.3.3 Darcy's law

Constitutive Darcy's law is presented in the expression,

$$q_w = -k_{wz} \nabla \left(\frac{u_w}{\rho_w g} \pm Z \right)$$

(2-8)

Whit,

q_w: water flux,

k_{wz}: permeability coefficient in direction z,

Z: distance to the datum level for the piezometric head.

Darcy's law does not establish a relationship between the velocity of the water that flows through the porous along the continuous medium and the actual area through which the water flow passes; this is because Darcy's laboratory test takes into account the area of the solid particles where there is no water flux.

Therefore, it is necessary to fix this relation considering the real area where the water goes through.

$$\overrightarrow{q_w} = A_r \overrightarrow{v_r}$$

(2-9)

With,

A_r: Real area where the water can go through. This means that water can pass just by throwing water,

$\overrightarrow{v_r}$: real velocity of the water throughout the soil.

If the soil is divided into infinite differential heights, the volumetric ratios of the distinct phases can be related to their area relations.

This means that,

$$A_W = V_w \, , A_v = V_v, A_s = V_s \tag{2-10}$$

Where,

A_w: Water area of the cross section in an unsaturated soil sample,

A_v: Void area of the cross section in an unsaturated soil sample,

A_s: Soil particles area of the cross section in a unsaturated soil sample.

And soil parameters that were previously characterized using volume phases are now defined using area phases.

$$\frac{A_w}{A_v} = \frac{V_w}{V_v} = Sr, \frac{V_v}{V_T} = n \tag{2-11}$$

Then we received,

$$\overrightarrow{q_w} = nS_r\overrightarrow{v_w} \tag{2-12}$$

Combining the expressions (2-7) and (2-12), it results possible to express water mass equation into terms of water flux q_w as shown in (2-13).

$$\frac{\partial(nS_r)}{dt} + \nabla(\rho_w\overrightarrow{q_w}) = 0 \tag{2-13}$$

Finally, replacing with the soil properties, finishes as,

$$\frac{\partial(nS_r)}{dt} + \nabla(\rho_w nS_r) = 0 \tag{2-14}$$

The term of ρ_w disappears when the density is considered as a constant.

2.3.4 Retention curve

In an unsaturated soil, there exists air-water interphases. These interfaces know surface tension resulting from intermolecular forces acting on molecules in the contractile skin (Figure -5). By setting force equilibrium of the menisci, surface tension can be related to the pressure difference $u_a - u_w$ existing in the air and water phases:

$$\Delta u = u_a - u_w = \frac{2T_s}{R_s} \tag{2-15}$$

where R_s is the radius of curvature of the menisci and T_s the surface tension (Figure 2-5).

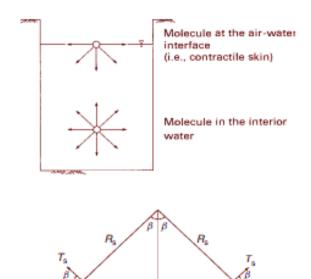Figure 2-5. Surface tension phenomenon at air-water interface. (a) Intermolecular forces acting on contractile skin. (b) Surface tension forces associated with curved two-dimensional surface. [4]

Suction is moreover related to the degree of saturation or water content inside the soil through the Soil-Water Characteristic Curve (SWCC). Water content is defined by:

$$\theta_w = \frac{V_w}{V_v + V_s} = nS_r \tag{2-17}$$

A typical curve for a SWCC is shown in Figure 2-6 and it is divided into three main zones.

The suction range below the air-entry value of the material remains essentially saturated. The zone between the air-entry value and before the residual degree of saturation where material properties, such as permeability, experiment nonlinear variation with degree of saturation. And the dry zone characterized by an essential immobile water linked to the particles.
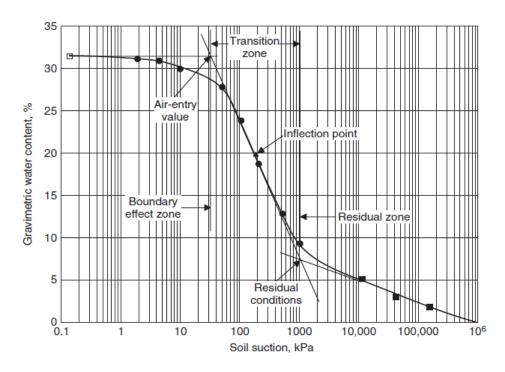
Figure 2-6.Typical desorption SWCC showing distinct zones of desaturation. [4]

In order to linearize the analysis, the degree of saturation S_r could be defined as the slope for a linear function of the SWCC. (see eq. (2-16))

$$S_r = \frac{u_a - u_w}{adu_W}$$

(2-16)

After using Darcy's law, the terms of degree of saturation can be represented in terms of the retention curve using the following expression, if the expression of mass conservations is to be specified in terms of water pressure.

$$a = \frac{dS_r}{du_w} \ [kPa]$$

(2-17)

22

Where $a < 0$ and is the slope of the retention curve in a singular tangent point of the function.

2.4   Derivation of the equation in terms of pressure

According to the retention curve slope, expressed in equation (2-17), results possible to introduce the water pore pressure into the water mass conservation equation.

Water flow rate across a unit area of the soil in one direction v_{wz} can be substituted with Darcy's law as,

$$v_{wz} = -\frac{k_{wz}(u_a - u_w)dh_w}{dz}$$
(2-18)

Where,

$k_{wz}(u_a - u_w)$: water coefficient of permeability which varies in the z direction since it is a function of matric suction.

Therefore, equation (2-14) ends as,

$$\frac{k_{wz}}{\rho_w na}\frac{\partial^2 h_w}{\partial z} = \frac{\partial h_w}{\partial t}$$
(2-19)

And substituting $z + u_w/\rho_w g$ for the hydraulic head h_w, equation (2-19) results,

$$\frac{\partial u_w}{\partial t} - \frac{k_{wz}}{na}\frac{\partial^2 u_w}{\partial Z^2} = 0$$
(2-20)

With κ as the diffusion coefficient for the PDE,

$$\kappa = \frac{k_{wz}}{na}$$
(2-21)

2.5   Derivation of the equations in terms of water content

It is also possible to substitute water content instead of suction in the mass balance equation, leading to the so-called Richard's equation [11]:

This results from,

$$\nabla(q_w) = \frac{\partial \theta_w}{\partial t} \qquad (2\text{-}22)$$

Where,

q_w : Darcy's law water flux

θ_w : Water content

And from eq. (2-12) and sink source considered as zero, volumetric water content changes on time as,

$$\nabla(nS_r \overrightarrow{v_w}) = \frac{\partial \theta_w}{\partial t} \qquad (2\text{-}23)$$

And then considering Darcy's law in terms of water content, Richards's theory equation is.

$$\frac{\partial \theta_w}{\partial t} - \kappa \frac{\partial^2 \theta_w}{\partial Z^2} = 0 \qquad (2\text{-}24)$$

Where

$$\kappa = \frac{k_w}{na} \qquad (2\text{-}25)$$

3 CHAPTER: APPOACHES FOR WATER CONTENT ESTIMATION

These chapter describes two methods to assess the variations of water content inside an unsaturated soil layer. These methods belong to the so-called Reduced Order Models in the sense that they use only partial information to do the prediction.

1) The first method consists in setting a statistical soil transfer function (SFT) by correlating the variation of water content at the target depth to the variation of water content at soil surface. Once set the transfer function on the basis of a limited period of the two time series, it is used to predict the variation of water content at the considered depth for the remaining part of the series. This exercise is done at each depth of water content monitoring.

2) The second method consists in deriving a deterministic SFT based on the analytical solution of the one-dimensional infiltration equation presented in Chapter 2. The analytical solution considered a constant diffusion coefficient and two boundary conditions: a periodic sinusoidal boundary condition at the top of the one-dimensional soil column and a null water content at the bottom.

Both methods are illustrated in Chapter 4 for the case of one test field located at "Le Fauga" site in France. The test field is now briefly described.

3.1   Presentation of the field experiment

The experiment is located at a site of the French National Service of Meteorology at "Le Fauga", Midi-Pyrénées – France (Figure 3.1).

The location and the stratigraphy of the experimental field is shown at Figure 3-1**Error! Reference source not found.** The soil is constituted by four different layers:

- Silt: 0 to 0.5 m
- Sandy: 0.5 to 2.0 m
- Gravel: 2.0 to 4.6 m
- Marl: 4.6 m downwards.

Atmospheric variables are monitored each 30 mins by a meteorological station. It includes measurements of precipitation, atmospheric pressure, incoming solar and atmospheric radiation, air temperature, air relative humidity, and finally wind speed and direction at 2 m.

Water contents and temperatures are monitored each 10 cm up to a depth of 1 m. Monitoring frequency is 30 mins.

Monitoring includes also estimation of sensible and latent heat flux across soil surface and vegetation parameters (biomass, dry matter, water content and Leaf Area Index).
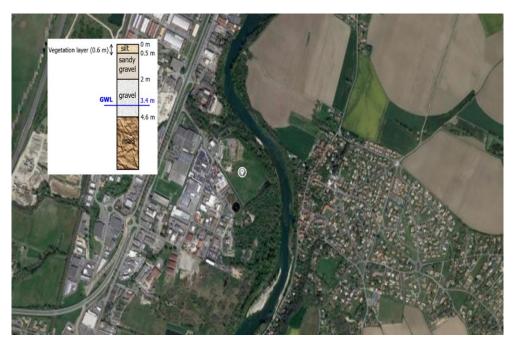
Figure 3-1. Field experiment location – N 43°28'37.92'', E 1°20'34.08''. Characteristic geotechnical units.

3.2   Method 1. Determination of the statistical soil transfer function

The statistical SFT is determined over a limited period extracted from the time series. As Fourier series decomposition will be used, the period must be selected such that both the input and output time series are stationary over the period.

1) Spectral decomposition of the time series monitored at depth z, noted *f(t) and* named hereinafter "Output"

$$f(t) = a_0 + \sum_{n=1}^{N} [a_n \cos(w_n t) + b_n \sin(w_n t)] \tag{3-1}$$

$$= \frac{A_0}{2} + \sum_{n=1}^{N} A_n \cos(w_n t + \phi_n) = \frac{A_0}{2} + \sum_{n=1}^{N} A_n \sin\left(w_n t + \phi_n + \frac{\pi}{2}\right)$$

with

$$A_0 = \frac{a_0}{2}$$

$$A_n = \sqrt{a_n^2 + b_n^2}$$

$$\phi_n = \tan^{-1}\frac{b_n}{a_n}$$

where

A_0: mean value of f(t,z)

A_n: n^{th} harmonic amplitude

ϕ_n: n^{th} phase shift

w_n: n^{th} harmonic angular frequency (Hz)

A_0, A_n, θ_n and w_n are coefficient characteristics of the considered depth z.

2) Determination of the spectra $A_n(\omega_n)$ and $\theta_n(\omega_n)$

3) Spectral decomposition of the time series monitored at soil surface, noted $f_0(t)$ and named hereinafter "Input".

$$f_0(t) = \frac{A_{00}}{2} + \sum_{n=1}^{N} A_{0n} \sin\left(w_{0n} t + \phi_{0n} + \frac{\pi}{2}\right) \tag{3-2}$$

where A_{00}, A_{0n}, ϕ_{0n} and w_{0n} are the mean value and n-harmonic of amplitude, phase shift and angular frequency of the time series at soil surface.

4) Determination of the spectra $A_{0n}(\omega_{0n})$ and $\phi_{0n}(\omega_{0n})$

5) Determination of the soil transfer functions for amplitude and frequency as the ratio between the output and input spectra:

$$SFT_A(\omega_n) = \frac{A_n(\omega_n)}{A_{on}(\omega_n)} \tag{3-3}$$

$$SFT_\theta(\omega_n) = \frac{\phi_n(\omega_n)}{\phi_{on}(\omega_n)}$$

The method will be illustrated on the basis of "Le Fauga" experimental data. Input corresponds to the water content at the shallowest depth (0.05 cm) while the Outputs are the time series at depth 0.15, 0.25, 0.35, 0.45, 0.55, 0.65, 0.75, 0,85 and 0.95 m (Figure 3-2). Series last for 7 years but only 6 years have been considered for the sake of series stationarity.

Measurements was store in a general matrix A, whose columns (10 in total) corresponds to the depth of the measurements and the line to the times. The 1st column corresponds to the input and the others to the output.
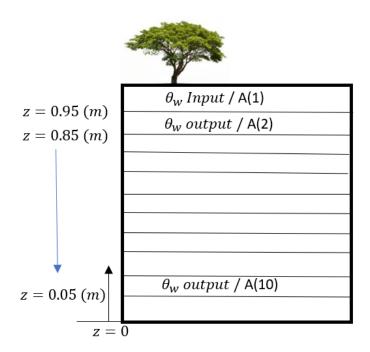
Figure 3-2. Data discretization in terms of input and output layers.

Matrix has been split in two equal parts of 3 years duration: A1 for calibration of the SFTs, and A2 for the prediction of water contents. To ensure that matrix A1 and A2 have the same harmonics as matrix A, a procedure adjustment has then been applied to the duration of both series. It consists of removing some data at the end of the series to optimize the match between A1/A2 and A harmonics.

In a first step, a Fast Fourier Transform has been applied to get the amplitude and phase spectra at each depth and compute the FFT_A and FFT_θ. It is expected that the main modes correspond to the typical meteorological cycles: year, half a year, month, and day.

Afterwards, the SFTs have been applied to the 1st column of the A2 matrix in order to obtain predicted spectra of water contents for the period under consideration. Finally, an inverse Fourier Transform has been applied to compute the time response of water content at the several depths and compare them with monitored measurements.

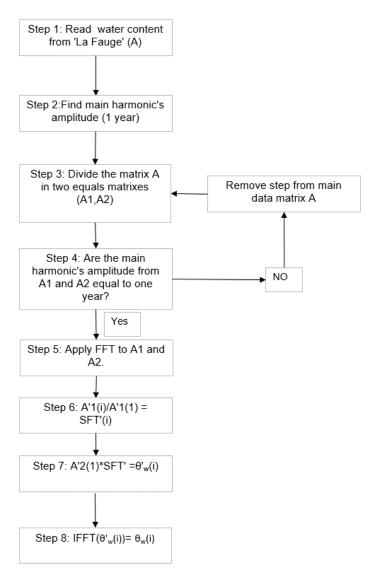Figure 3-3 presents a flowchart that summarizes the steps carried out.

Figure 3-3. Flowchart of the algorithm to estimate water content θ_w

3.3 Method 2. Determination of the deterministic soil transfer function

The second method consists in computing the STF using the analytical solution of the one-dimensional infiltration equation discussed in Chapter 2.

The general PDE reads as:

$$\frac{\partial u}{\partial t} = \kappa^2 \frac{\partial^2 u}{\partial x^2} \qquad (3\text{-}4)$$

Where u can be alternatively pore pressure or water content.

The problem under consideration corresponds to the case of a unidimensional soil column under periodic boundary condition and a fixed water table at L meters depth (Figure 3-4). At the bottom, a pore pressure equal to 0 or a constant water is prescribed. The periodic boundary condition is represented by a periodic function with amplitude A_k, angular frequency w_k and phase ϕ_k. Index k indicates that the condition corresponds to a given mode. For general conditions, such as the ones prescribed by a climatic action, several modes will be superimposed.

Mathematically, for a given mode, the problem gets expressed as:

$$\frac{\partial u}{\partial t} = \kappa \frac{\partial^2 u}{\partial x^2} \qquad (3\text{-}5)$$

with

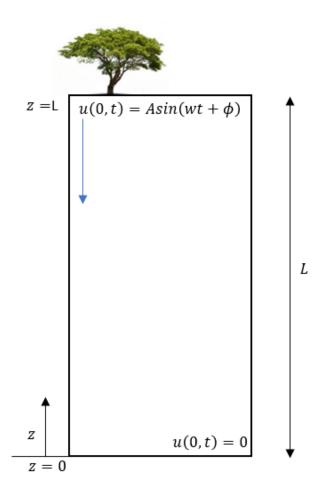|	
$u = 0$	for $x = 0$ and $\forall\, t$
$u = A_k sin(w_k t + \phi_k)$	for $x = L$ and $\forall\, t$
$u = f(x)$	$\forall\, x$ and for $t = 0$

Figure 3-4. Schema of the proposed diffusion problem.

Considering an initial pore pressure distribution that varies linearly from u_{01} at $x = 0$ to u_{02} at $x = L$

$$f(x) = u_{01}\left(1 - \frac{x}{L}\right) + u_{02}\frac{x}{L}$$

(3-6)

The solution for the problem includes a transient term and a term due to the periodic action:

(3-7)

$$u(x,t) = \sum_{n=1}^{\infty} A_n \, sin\left(\frac{n\pi x}{L}\right) e^{-\kappa\left(\frac{n\pi}{L}\right)^2 t}$$
$$+ A_k \frac{(e^{\alpha_k x} - e^{-\alpha_k x})}{(e^{\alpha_k L} - e^{-\alpha_k L})}[sin\,(w_k t + \phi + \alpha_k(x - L)]$$

where

$$A_n = \int_0^L f(x) \sin\left(\frac{n\pi x}{L}\right) dx$$

and

$$\alpha_k = \sqrt{\frac{w_k}{2\kappa}}$$

Fig 3-5 schematically shows the variation of pore pressure or water content resulting from the attenuation in amplitude and shift in phase outcoming from this diffusion character of the infiltration solution.

For a condition involving N modes k, the solution will be:

$$u(x,t) = \sum_{n=1}^{\infty} A_n \sin\left(\frac{n\pi x}{L}\right) e^{-\kappa\left(\frac{n\pi}{L}\right)^2 t} \tag{3-8}$$

$$+ \sum_{k=1}^{N} A_k \frac{(e^{\alpha_k x} - e^{-\alpha_k x})}{(e^{\alpha_k L} - e^{-\alpha_k L})} [\sin(w_k t + \phi_k + \alpha_k(x-L))]$$

According to equation (3-8), the SFTs for a stationary input (i.e. without transient term) are:

$$SFT_A : A_k(w_k, x) = \frac{(e^{\alpha_k x} - e^{-\alpha_k x})}{(e^{\alpha_k L} - e^{-\alpha_k L})}$$

$$SFT_\phi : w_k \to \phi_k(w_k, x) = \phi_k + \alpha_k(x-L) \tag{3-9}$$

SFTs can then be used to predict the response at depth from the response in surface. The steps are the following:

1) Compute the amplitude and phase spectra for the response in surface by using the Fast Fourier Transform
2) Apply the SFTs functions to the amplitude and phase spectra at each step
3) Apply the inverse Fourier transform to obtain the response in the time domain at each depth.

Procedure can be directly applied to the input series provided that parameters κ and L are known. If not, the procedure can be trained on a partial set of monitored series to obtain κ and

L that minimize the error between computed and measured data. The effect of increasing the length of the column is schematically depicted in Fig. 3-6.
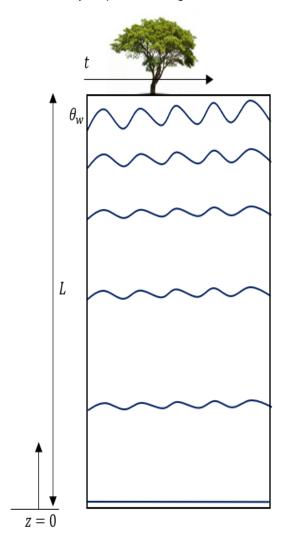

Figure 3-5. Water content distribution considering a null border condition at the bottom of one-dimensional soil column in time.

Finally, the analytical solution does not consider any constant term as is the sum of pair function (sin) and the prediction must be shifted by the mean value of water content of the series at the considered depth. The shift term, labelled A0 is the third parameter entered in the training process. The method is illustrated in Chapter 4 using the monitored data at "Le Fauga".
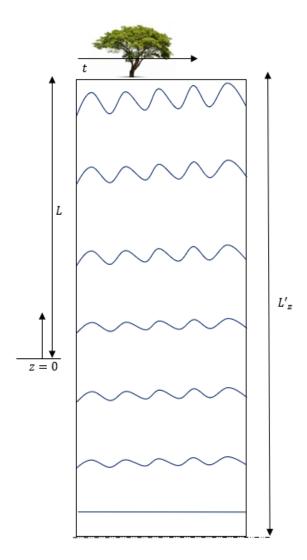
Figure 3-6. Expected water content distribution optimizing the length L'_z for the analytical solution of diffusion equation in a one-dimensional soil column in time

4 CHAPTER: WATER CONTENT ESTIMATION RESULTS

In this chapter, based on the approaches presented in section 3, it will be performed a water content estimation. To do so, a set of recorded data will be used as a case of study.

4.1 Water content records from 'Le Fauga'.

In this section, the recorded data of water content θ_w during seven years at several depths will be analyzed. These records are presented in Figure 4-1 and Figure 4-2. Note that the distribution of the water content follows a periodical pattern along the one-dimensional soil column
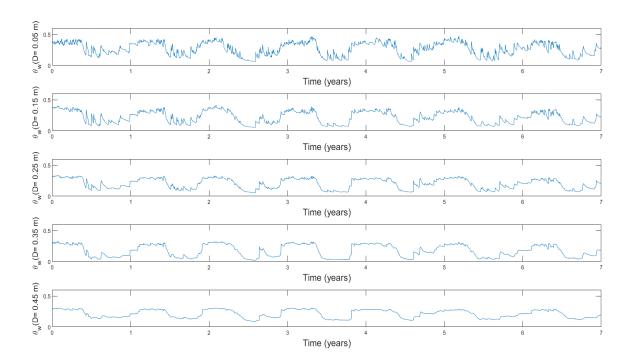

Figure 4-1. Water content θ_w for measured depth from 0.05 cm to 0.45 cm below surface.
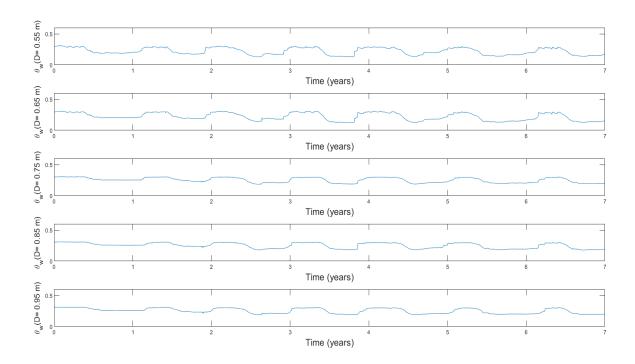
Figure 4-2. Water content θ_w for measured depth from 0.55 cm to 0.95 cm below surface.

From Figure 4-1 and Figure 4-2., it is possible to verify that the water content near the surface is more dependent from environmental processes such as evaporation, wind, solar radiation, etc. At greater depths, the evolution of this variable becomes smooth. This indicates that the frequency content of the variable at greater depths will be governed by few harmonics in a Fourier series.

Furthermore, from the representation of the recorded data, it is possible to observe that the water content suffers a delay in time along depth. However, it does not affect the identification of the principal harmonics of the signal. For instance, if the amplitude spectra is obtained for all the signals shown in Figure 4-1 and Figure 4-2, it can be seen that the main harmonics have a fundamental frequency of approximately one year (see Figure 4-3). Particularly, in Figure 4-3, it is possible to observe that the highest peak is for 8756.57 hours or 364.85 days. It occurs for all depths. This shows that the fluctuations of the water content of the soil are strongly tied to those related to the climatic variables. The latter also exhibit a fundamental harmonic of one year.
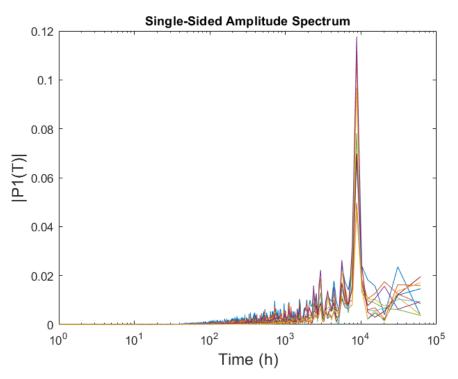
Figure 4-3.Amplitude spectrum in time (hours) for the measurements at 'Le Fauga'

4.2   Prediction of water content variations with SFT

According to the procedure presented in chapter 3 based on transfer functions, the original data from 'Le Fauga' has been divided in two subsets. Each of them contains about half of the data. The first subset is used to compute the SFTs at every depth. Based on these functions, the water content of the second half of data can be predicted.

However, due to the periodic nature of the analysed data, phase problems may arise. Thus, it is necessary to ensure that the data of both new signals have similar phases. In this way, the main harmonics of both signals will have a similar period, as expected. It is also important to verify that both periods are not only similar to each other but also close to one year.

In line with the above, it has been carried out a procedure to obtain two subset of signals with similar phases, and fundamental periods around one year. To do so, the following procedure has been employed:

1.   Divide the signal in two subsets and calculate the amplitude spectrum.
2.   Identify the fundamental period of the main harmonic in both signals.
3.   Verify two aspects: i) are both periods similar? ii) are both periods close to one year?.

4. If the conditions presented in step 3 are fulfilled, the resultant signals are used to perform the transfer functions analysis. Otherwise, remove the last two points from the entire data set and repeat steps 1-3 until these conditions are reached.

Thus, in Figure 4-4, the blue and orange lines represent the frequency at which the amplitude spectra of the signal for the first and second subsets of data, respectively, are maxima. The yellow line represents one year. Accordingly, the first intersection of these three lines is when 19210 of 122592 time steps are removed. There are other solutions that meet the above conditions, but they have been ruled out as they involve removing a greater number of points.
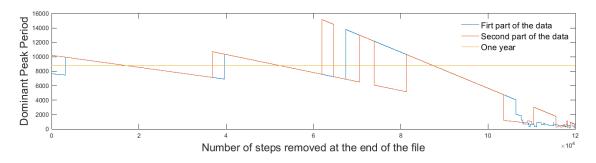

Figure 4-4. Dominant peak path in function of the steps removed.

For the sake of convenience, with each of the subsets generated in the iterative procedure described above, it has been performed a verification of the predictive capacity based on transfer functions. Thus, for each iteration, the predictive capacity of the first subset to estimate the evolution of the second has been measured. It has been done by calculating the coefficient of determination between the prediction and the observed data. Note that there will be a coefficient of determination for each layer. Accordingly, it has been analysed the evolution of the average of the entire group of coefficients of determination, $\bar{R}^2$. In Figure 4-5, it can be seen that the average correlation associated to the first solution identified in Figure 4-4 is significant (i.e. $\bar{R}^2 > 0.8$).

Figure 4-5. Optimization curve for the number of steps removed.
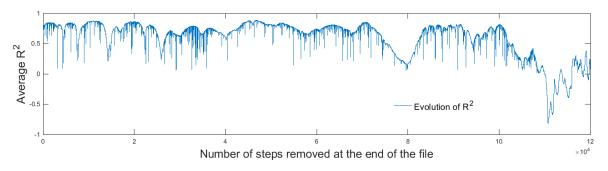
38

Thus, Figure 4-6 and Figure 4-7 shows the water content evolution for the subset A1 and subset A2, respectively.

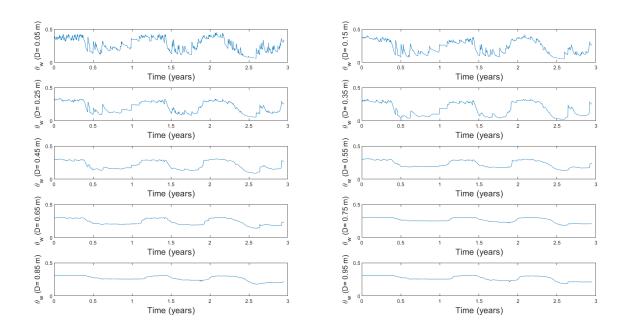Figure 4-6. First subset of the evolution of the water content θ_w (used to develop transfer functions)
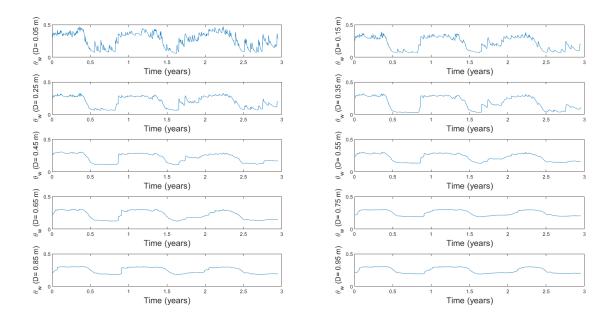
Figure 4-7. First subset of the evolution of the water content θ_w (used to test the predictive power of the transfer functions)

Following the procedure described in the flowchart shown in Figure 3-3**Error! Reference source not found.**, the blue line in Figure 4-8 represents the water content estimated from the SFT approach, while the orange line represents the water content measured in-situ.

Figure 4-8. Water content θ_w predicted from SFT obtained by data measurements.

The absolute difference between both predicted and recorded data is depicted in Figure 4-9.

Figure 4-9.Absolute difference for the SFT water content prediction in time.

4.3   Estimation of water content variations based on the analytical solution

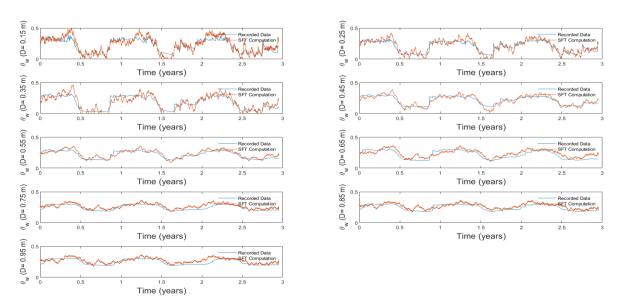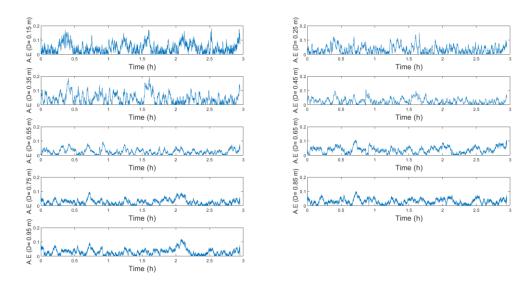As it was explained in section 3, to estimate the water content in a one-dimensional soil column using the analytical solution for the diffusion equation, it is necessary to propose an initial value for the intrinsic soil parameter κ and the independent Fourier's value A_0.

Additionally, the analytical solution assumes that the water content varies from a specific value close to the surface until zero at a specific depth. However, at the maximum depth of the recorded data, the water content is not zero. Thus, it is necessary to find an equivalent length of the profile, L_{zp}, so that the value at the maximum depth will not be zero.

In order to solve this issues, it has been analysed the mean square error, MSE, between the analytical solution and the measured values. The MSE is obtained for values of κ and L_{zp} in the range 0.0002-0.01 and 1-2, respectively. Again, there will be as many MSE values as records. For the sake of simplicity, the average value of the MSE at all depths is presented in Figure 4-10. The darker blue area represents the optimal combination of values, κ and L_{zp}, that minimize the MSE compared to the recorded water content data over time. The optimal values for κ and L_{zp} are 0.001 and 1.6 m, respectively.

It is worth mentioning that the A_0 values for each solution have been obtained from the recorded data (see Figure 4-11). From Figure 4-11, it can be observed that A_0 decreases linearly up to roughly 0.35 m from the surface. This could imply that there is a change in the hydrological qualities of the soil or factors outside the scope of this investigation below this level.
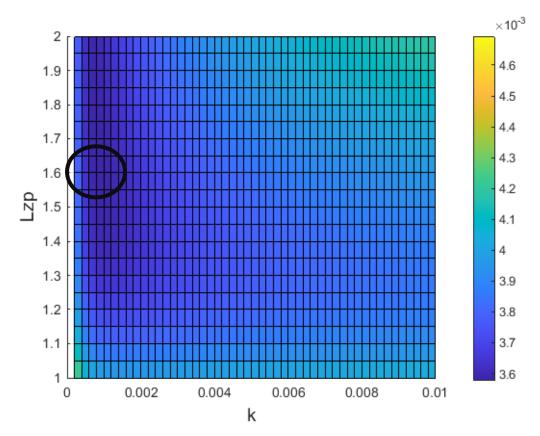
Figure 4-10. Mean squared error (MSE) surface for the soil parameters κ and L_z'

Based on the analytical solution, the best κ and L_{zp}, and using the values provided in Figure 4-11 for the independent term, it has been estimated the evolution of the water content. Figure 4-12 shows a comparison between both the recorded data and the analytical solution. It can be seen the good agreement for all depths.
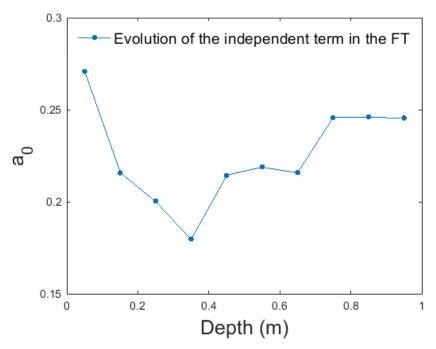
Figure 4-11. Evolution of the independent term A_0 from 'La Gauge' measurements
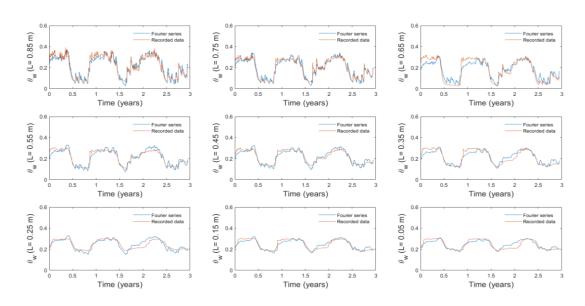
Figure 4-12. Fourier series computation adding A_0 knowing the respond of the system.

Another approach to estimate A_0 is to assume that it will be constant at all depths and equal to the one recorded close to the surface. However, higher errors are observed based on this approach (see Figure 4-13).
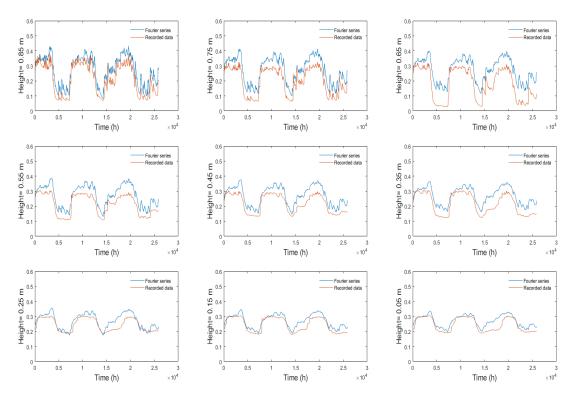
Figure 4-13. Fourier series computation adding A_0 as a constant.

In order to compare both considerations about A_0, as a constant and knowing the respond of the system, Figure 4-14 includes the recorded data and both approaches.
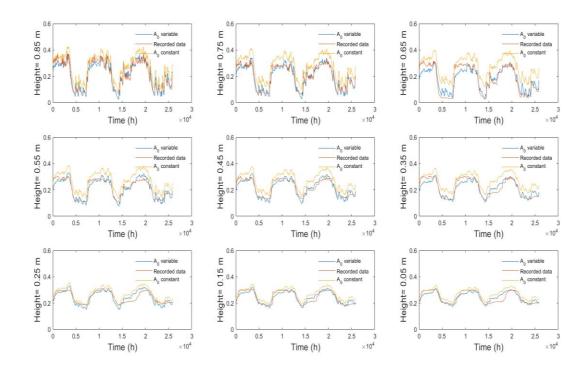
Figure 4-14. Fourier series computation adding A_0 as a constant and knowing the respond of the system.

In Figure 4-15 is represented the absolute difference between the recorded data and the water estimation adding an A_0 knowing the respond of the system. If it is compared with Figure 4-16, it is possible to verify the higher error when A_0 is considerer as a constant.
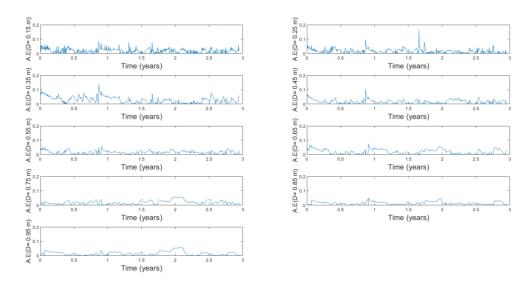
Figure 4-15.Absolute difference computation adding A_0 knowing the respond of the system.
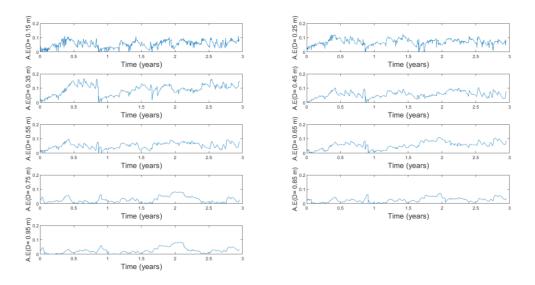
Figure 4-16.Absolute difference computation adding A_0 as a constant.

5 Conclusions

Weather conditions are typically associated with ground surface instability. Most superficial layers are likely to have varying water contents and are frequently unsaturated and changes in pore pressure or water content in a soil column are caused by environmental variables interacting with the most superficial ground layer.

As was previously indicated, in order to assess groundwater fluctuations and predict future water changes, it is occasionally essential to continue with hydrological studies that span broad areas and take some time to finish.

The primary goal was to use two rapid methods of spectral analysis were for estimating the water content in a one-dimensional soil column.

The first method consisted in setting a statistical soil transfer function (SFT) by correlating the variation of water content at the target depth to the variation of water content at soil surface. Once was set the transfer function on the basis of a limited period of the two time series, it was used to predict the variation of water content at the considered depth for the remaining part of the series. This exercise was done at each depth of water content monitoring

It was determined throughout the investigation that a statistical SFT requires previous measurements in the soil column at different depths for at least a year. With fewer readings, it would be impossible to identify the data series' prominent harmonics, and this amount of time measures makes it possible.

The last assertion only applies to latitudes where the environment exhibits seasonal patterns such in "Le Gauge." Finding the major harmonic's amplitudes period would be necessary to respond to the procedure if it were reproduced in a latitude where it does not follow a different seasonal behavior.

The water mass balance, Darcy's law and the Soil-Water Characteristic Curve (SWCC) were used to obtain a water mass balance expression in connection to water pressure and water content. As it is shown in Figure 2-6, SWCC follows a non-linear curve. For this investigation, the slope a of SWCC was considered as lineal and in function of the variation of degree of saturation and variation of pore pressure.

The combination of the three final governing equations allowed the development of a partial differential equation known as the diffusion equation. The diffusion coefficient considers soil porosity, while the SWCC linearizes slope.

Furthermore, the analytical solution for the diffusion equation for a sinusoidal boundary condition at the top of the one-dimensional soil column and a zero amount of water at the bottom was obtained.

Then, the second method of spectral analysis consisted in deriving a deterministic SFT based on the analytical solution of the one-dimensional infiltration equation presented in Chapter 2. The analytical solution considered a constant diffusion coefficient and two boundary conditions: a periodic sinusoidal boundary condition at the top of the one-dimensional soil column and a null water content at the bottom.

Following the study of the water content data, the soil column required to be corrected with a new length L'_z assumed for the diffusion equation. This could have been prevented if the border condition had not been null at the bottom. Further investigation should involve boundary condition correction in order to improve the efficiency of computational calculations.

To estimate the water content, the water content function, exposed in section 303.3, required three values: the independent Fourier's series value A_0, the diffusion coefficient κ, and the adjusted new length for the analytical diffusion equation solution L'_z.

Despite the fact that the analytical diffusion equation solution strategy is to estimate the water content signal from just an input water content layer, knowing the respond of the system was required identify κ and L'_z

The diffusion coefficient κ is equal to 0.001 and the corrected new length L'_z is 1.6 m, according to the optimization for the analytical solution parameters. (Figure 4-10)

Both estimating methods revealed a decreasing absolute difference with the monitored water content at 'Le Fauga', as one moved further down the one-dimensional soil column. The various environmental interactions that affect the most superficial soil layer can explain the higher water content prediction error.

Results shown that the estimation of water content using a deterministic soil transfer reached higher accuracy provided that the procedure is trained on a sub-set of measurements in order to determine characteristics values for the equation control parameters (length of the column, diffusion coefficient).

The independent Fourier's value A_0 was supposed to have a lineal decline across depth. It is feasible to see from Figure 4-11 that the mean value A_0 has a parabolic tendency. The cause for the curve's non-linearity can be explained by variations in the intrinsic parameters along the soil column where the measurements were taken, or by any unknown water source.

More site studies to parametrize the diffusion coefficient and calibrate the analytical solution to estimate the water content using historical water content records in the topmost layers of the ground are possible next steps in further research.

A hazard assessment model was proposed by Gitirana and Fredlund [3]for embankment analysis. This model integrates unsaturated soils properties related to the SWCC. A dynamic programming optimization was used to determine the slope stability conditions. The stability of an embankment is related to the reduction in matric suction within the embankment
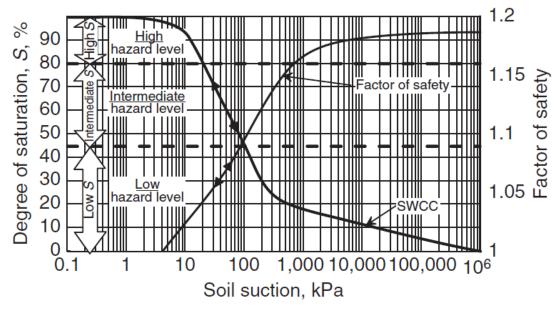

Figure 5-1. SWCC as water level gauge and embankment hazards gauge [4].

Spectral analysis of soil water content can help in estimating water content and periodic frequency water fluctuations. This can provide a measure of stability (i.e., the factor of safety) and model the possibility of future geohazards.

References

[1] H. Dregne, Soils in Arid Regions, New York: Elsevier, 1976.

[2] D. Chen, Y. Li, R. E. White, A. Zhu and J. Zhang, "Estimating soil hydraulic properties of Fengqiu County soils in the North China Plain using pedotransfer functions," no. Elsevier Editorial System Geoderma , pp. 261-274, 2007.

[3] J. Gitirana and D. Fredlund, "Experimental evidences towards the assessment of weather-related railway embankment hazards," in *Proceedings of the International Conference on the Theme "From Experimental Evidences Towards Unsaturated Soil Practice"*, Weimar, Germany, 2003b.

[4] H. R. a. M. F. D.G. Fredlund, Unsaturated Soil Mechanics in Engineering Practice, WILEY, 1940.

[5] H. Bouver, Groundwater Hydrology, New York: McGraw-HIll, 1978.

[6] D. Croney, J. Coleman and W. Black, "Movement and distribuition of water in soil in relation to highway design and performance," *Water and Its Conduction in Soil,* p. 252, 1958.

[7] S. Samat and J. Vaunat, "Environmental Actions on Slope Responses," in *Code_Bright Workshop*, Barcelona, 2011.

[8] J. Bear, Dynamics of Fluids in Poroues Media, New York: American Elsevier Publishing Company, 1972.

[9] G. Blight, Mechanics of Resigual Soils, Rotterdam : Balkema, 1997.

[10] C. J, The Mathematics of Diffusion, London: Oxford University Press, 1975.

[11] L. Richards, "Capillary conduction of liquids through porous mediums," *Physics 1,* no. https://aip.scitation.org/doi/10.1063/1.1745010, pp. 318 - 333, 1931.

[12] V. PJ, "Editorial: Soil-atmosphere interaction," no. http://doi.org/10.1680/jenge.2019.6.6.320.

[13] M. Frigo and S. Johnson, "FFTW: An Adaptive Softwater Architecture for the FFT," *Proceedings of the International Conference on Acoustics, Speech, and Singal Processing,* vol. 3, pp. 1381 - 1384, 1998.

[14] D. P and M. Vetterli, "Fast fourier transforms: A tutorial review and state of the art," *Signal Processing,* vol. 19, no. 4, pp. 259 - 357, 1990.

Appendix A. Diffusion equation developed solution

Diffusion equation solution under periodic boundary conditions.

The problem reads:

$$\frac{\partial u}{\partial t} = k \frac{\partial^2 u}{\partial x^2}$$

with: $u = 0$ for $x = 0$ and $\forall\, t$ A- 1

$u = A sin(wt + \phi + \frac{\pi}{2})$ for $x = L$ and $\forall\, t$

$u = f(x)$ $\forall x$ and for $t = 0$

Find $z \in \mathbb{C}$ such that

$$U_s(x,t) = \Im\left(\frac{e^{zx} - e^{-zx}}{e^{zL} - e^{-zL}} A e^{i(wt+\phi)}\right) \qquad \text{A- 2}$$

Satisfies the equation and the boundary conditions (but not the initial conditions). Then the problem satisfied by

$$V(x,t) = U(x,t) - U_s(x,t) \qquad \text{A- 3}$$

To get the value of z, let us compute

$$\left(U_s(x,t)\right)_t = \Im\left(\frac{e^{zx} - e^{-zx}}{e^{zL} - e^{-zL}} A i e^{i(wt+\phi)}\right) \qquad \text{A- 4}$$

And

$$\left(U_s(x,t)\right)_{xx} = \Im\left(z^2 \frac{e^{zx} - e^{-zx}}{e^{zL} - e^{-zL}} A e^{i(wt+\phi)}\right) \qquad \text{A- 5}$$

Hence if one chooses $iw = kz^2$, the equation $\left(U_s(x,t)\right)_t = \left(U_s(x,t)\right)_{xx}$ is satisfied.
Assuming w and k are positive, it follows that

$$z = -\pm \sqrt{\frac{w}{2k}}(1+i)$$

$$\alpha = \sqrt{\left(\frac{w}{2k}\right)}$$

$$U(x,t) = \sum_{n=1}^{\infty} \int_0^L f(x)\sin\left(\frac{n\pi x}{L}\right) dx \sin\left(\frac{n\pi x}{L}\right) e^{-k\left(\frac{n\pi}{L}\right)^2 t}$$

$$+ \ \Im\left(\frac{e^{zx} - e^{-zx}}{e^{zL} - e^{-zL}} Ae^{i(wt+\phi)}\right)$$

$$\Im\left(\frac{e^{zx} - e^{-zx}}{e^{zL} - e^{-zL}} Ae^{i(wt+\phi)}\right)$$

$$\left[\frac{e^{\alpha(1+i)x} - e^{-\alpha(1+i)x}}{e^{\alpha(1+i)L} - e^{-\alpha(1+i)L}}\right] Ae^{i(wt+\phi)}$$

$$\left[\frac{e^{\alpha x}(\cos\alpha x + i\sin\alpha x) - e^{-\alpha x}(\cos\alpha x + i\sin\alpha x)}{e^{\alpha L}(\cos\alpha L + i\sin\alpha L) - e^{-\alpha L}(\cos\alpha L + i\sin\alpha L)}\right] Ae^{i(wt+\phi)}$$

$$\left[\frac{\cos\alpha x\,(e^{\alpha x} - e^{-\alpha x}) - i\sin\alpha x\,(e^{\alpha x} - e^{-\alpha x})}{\cos\alpha L\,(e^{\alpha L} - e^{-\alpha L}) - i\sin\alpha L\,(e^{\alpha L} - e^{-\alpha L})}\right] Ae^{i(wt+\phi)}$$

Using the following auxiliar variables to find the expression with the form $M + iN$

$$a = \cos\alpha x\,(e^{\alpha x} - e^{-\alpha x})$$
$$b = \sin\alpha x\,(e^{\alpha x} - e^{-\alpha x})$$
$$c = \cos\alpha L\,(e^{\alpha L} - e^{-\alpha L})$$
$$d = \sin\alpha L\,(e^{\alpha L} - e^{-\alpha L})$$

We got,

$$\left[\frac{a - ib}{c - id}\right] Ae^{i(wt+\phi)}$$

$$\left[\frac{a - ib}{c - id} \cdot \frac{c + id}{c + id}\right] Ae^{i(wt+\phi)}$$

$$\left[\frac{(a - ib) \cdot (c + id)}{c^2 - (id)^2}\right] Ae^{i(wt+\phi)}$$

$$\left[\frac{ac + iad - ibc + bd}{c^2 + d^2}\right] Ae^{i(wt+\phi)}$$

$$\left[\frac{ac + bd}{c^2 + d^2} + i\frac{ad - bc}{c^2 + d^2}\right] Ae^{i(wt+\phi)}$$

$$[M + iN] \cdot A(\cos(wt + \phi) + i\sin(wt + \phi))$$

$$[M + iN] \cdot (A\cos(wt + \phi) + iA\sin(wt + \phi))$$

$$(AM \cos(wt + \phi) + iAM\sin(wt + \phi) + iAN \cos(wt + \phi) - AN\sin(wt + \phi))$$

$$A(M \cos(wt + \phi) - N \sin(wt + \phi)) + i(AM \sin(wt + \phi) + AN \cos(wt + \phi))$$

Therefore, the imaginary part of the expression $\left(\frac{e^{zx} - e^{-zx}}{e^{zL} - e^{-zL}} A e^{i(wt+\phi)}\right)$ is

$$(A\frac{ac + bd}{c^2 + d^2} \sin(wt + \phi) + A\frac{ad - bc}{c^2 + d^2} \cos(wt + \phi))$$

$$\frac{A}{c^2 + d^2} \cdot [(ac + bd) \cdot \sin(wt + \phi) + (ad - bc) \cdot \cos(wt + \phi)]$$

$$\frac{A}{\left(\cos \alpha L \left(e^{\alpha L} - e^{-\alpha L}\right)\right)^2 + \left(\sin \alpha L \left(e^{\alpha L} - e^{-\alpha L}\right)\right)^2}$$
$$\cdot \Big[\left(\cos \alpha x \left(e^{\alpha x} - e^{-\alpha x}\right) \cos \alpha L \left(e^{\alpha L} - e^{-\alpha L}\right)\right.$$
$$+ \sin \alpha x \left(e^{\alpha x} - e^{-\alpha x}\right) \sin \alpha L \left(e^{\alpha L} - e^{-\alpha L}\right)\big) \cdot \sin(wt + \phi)$$
$$+ \left(\cos \alpha x \left(e^{\alpha x} - e^{-\alpha x}\right) \sin \alpha L \left(e^{\alpha L} - e^{-\alpha L}\right)\right.$$
$$\left. - \sin \alpha x \left(e^{\alpha x} - e^{-\alpha x}\right) \cos \alpha L \left(e^{\alpha L} - e^{-\alpha L}\right)\right) \cdot \cos(wt + \phi)\Big]$$
$$\frac{A(e^{\alpha x} - e^{-\alpha x})}{(e^{\alpha L} - e^{-\alpha L})} \Big[\left(\sin(wt + \phi)\left(\cos \alpha x \cdot \cos \alpha L + \sin \alpha x \cdot \sin \alpha L\right)\right)$$
$$+ \cos(wt + \phi)\left(\cos \alpha x \cdot \sin \alpha L - \sin \alpha x \cdot \cos \alpha L\right)\Big]$$
$$\frac{A(e^{\alpha x} - e^{-\alpha x})}{(e^{\alpha L} - e^{-\alpha L})} [\sin(wt + \phi + \alpha(x - L)]$$

Therefore,

The final solution for the equation A- 1 ends as,

$$U(x,t) = \sum_{n=1}^{\infty} \int_0^L f(x)\sin\left(\frac{n\pi x}{L}\right) dx \sin\left(\frac{n\pi x}{L}\right) e^{-k\left(\frac{n\pi}{L}\right)^2 t} + \frac{A(e^{\alpha x} - e^{-\alpha x})}{(e^{\alpha L} - e^{-\alpha L})} [\sin(wt + \phi + \alpha(x - L)] \qquad \text{A-6}$$